Fungal Biology 123 (2019) 709–722

Contents lists available at ScienceDirect

Fungal Biology

journal homepage: www.elsevier.com/locate/funbio

Subunits of the vacuolar H+-ATPase complex, Vma4 and Vma10, are essential for virulence and represent potential drug targets in *Candida albicans*

Se Woong Kim [a, b], Young Kwang Park [a, b], Yoo Jin Joo [a], Yu Jin Chun [a], Ju Yeon Hwang [a], Je-Hyun Baek [a], Joon Kim [a, b, *]

[a] Laboratory of Biochemistry, Division of Life Sciences, Korea University, Seoul, 02841, Republic of Korea
[b] HAEL Lab, TechnoComplex, Korea University, 145, Seoul, 02841, Republic of Korea

ARTICLE INFO

Article history:
Received 21 February 2019
Received in revised form
20 May 2019
Accepted 3 June 2019
Available online 12 June 2019

Corresponding Editor: Julian Rutherford

Keywords:
C. albicans
Candida drug
Morphogenesis
Pathogenesis
V-ATPase

ABSTRACT

Hyphal morphogenesis of *Candida albicans* is important for its pathogenesis. Here, we showed that the filamentous growth of *C. albicans* requires vacuolar H^+-ATPase function. Results showed that levels of Vma4 and Vma10 increased in cells undergoing hyphal growth compared to those undergoing yeast growth. Deleting *VMA4* or *VMA10* abolished vacuolar functions and hyphal morphogenesis. These deletion mutants were also characterized as avirulent in a mouse model of systemic infection. Furthermore, *VMA4* and *VMA10* deletion strains showed hypersensitivity to fluconazole, terbinafine, and amphotericin B. Based on these findings, Vma4 and Vma10 are not only involved in vacuole biogenesis and hyphal formation, but also are good targets for antifungal drug development in *C. albicans*.
© 2019 British Mycological Society. Published by Elsevier Ltd. All rights reserved.

1. Introduction

Candida albicans is an opportunistic human pathogen and a leading cause of hospital-acquired infections (Pfaller and Diekema, 2007). *C. albicans* is a major cause of bloodstream infection in both immunocompetent and immunocompromised individuals (Low and Rotstein, 2011). These infections are especially severe in immunocompromised patients with HIV, diabetes, cancer, or organ transplants (Fishman and Rubin, 1998). In addition, *C. albicans* can cause severe sepsis and septic shock (Duggan et al., 2015). *C. albicans* expresses several virulence factors that contribute to its pathogenesis such as the ability to change its morphology, secrete proteases, and form biofilms (Calderone and Fonzi, 2001; Kim and Sudbery, 2011; Santos et al., 2018; Sudbery, 2011).

The fungal vacuole is an acidic compartment containing a variety of hydrolytic enzymes that are important for cellular metabolite storage, osmoregulation, homeostasis, and detoxification (Li and Kane, 2009; Teter and Klionsky, 2000). V-ATPase is a member of the family of proton-translocation ATPases. In yeasts, V-ATPase generates a proton gradient that enables other membrane-bound transport systems to drive the accumulation of ions, small molecules, amino acids, and metabolites into the vacuole (Parra et al., 2014; Zhang et al., 1998). V-ATPase is composed of two domains: a peripheral V_1 domain (composed of eight subunits, A–H) and a membrane-embedded V_0 domain (composed of six subunits: a, d, e, c, c', c'') (Forgac, 2007; Olsen, 2014; Parra et al., 2014). The V_1 domain is a soluble catalytic sector that disengages easily depending on the cell conditions (Oot and Wilkens, 2010). This domain contains the catalytic subunits such as Vma4 and Vma10, which are responsible for ATP hydrolysis at the cytosolic side of the vacuolar membrane. The V_0 domain is embedded in the vacuolar membrane and contains the site of proton transport. Mutations of V-ATPase have shown a *vma*$^-$ phenotype that is characterized by poor growth in alkaline pH, defective metal sequestration, glycerol metabolism, and responses to many environmental stress conditions (Patenaude et al., 2013; Poltermann et al., 2005; Rane et al., 2013, 2014).

* Corresponding author. Laboratory of Biochemistry, Division of Life Sciences, Korea University, Seoul, 02841, Republic of Korea. Fax: +82 2 927 9028.
E-mail address: joonkim@korea.ac.kr (J. Kim).

https://doi.org/10.1016/j.funbio.2019.06.002
1878-6146/© 2019 British Mycological Society. Published by Elsevier Ltd. All rights reserved.

Several subunits of V-ATPase were investigated to determine their contributions to virulence-related traits in *C. albicans*. A recent study showed that V-ATPase pumps containing Vph1 or Stv1 contribute differently to *C. albicans* cell biology and virulence-related traits (Raines et al., 2013). Other studies on the V-ATPase subunits Vma3, Vma2, and Vma1 suggest that V-ATPase activity is a central requirement for filamentation, autophagy induction, and virulence in *C. albicans* (Jia et al., 2014; Rane et al., 2013, 2014).

V-ATPase is a fascinating target for drug discovery and there are numerous lines of evidence supporting a critical role for V-ATPase in *C. albicans* virulence (Olsen, 2014). V-ATPase inhibitors, such as bafilomycin A1 or concanamycin A, have been studied for their functions and mechanisms for over 20 y. Recently, Hayek et al. developed a high-throughput screening method to identify new V-ATPase inhibitors (Hayek et al., 2014).

In this study, highly expressed proteins in hyphal growing cells compared to yeast growing cells were identified using two-dimensional (2D) polyacrylamide gel electrophoresis (PAGE) and proteomic approaches. Among the identified proteins, we focused on Vma4 and Vma10, which are the putative E and G subunits of V-ATPase, respectively. Through genetic and molecular analyses, it was revealed that Vma4 and Vma10 are important for morphogenesis, virulence, and the physiological function of the *C. albicans* vacuole. These data present several lines of evidence that fungal V-ATPase and vacuoles play essential roles in germ tube formation and pathogenesis of *C. albicans*.

2. Materials and methods

2.1. Strains and growth conditions

All strains used in this study are listed in Table 1. All *C. albicans* strains were cultured in yeast extract-peptone-dextrose (YPD) medium (1 % yeast extract, 2 % peptone, 2 % dextrose). A synthetic complete medium (0.76 % yeast nitrogen base without amino acids, 2 % dextrose), supplemented with the appropriate auxotrophic requirements and uridine (50 μg/ml), was used to select positive transformants. To induce hyphal growth in a liquid medium, cells were grown overnight in YPD at 30 °C and re-cultured in YPD supplemented with 10 % serum (YPD-fetal bovine serum media), at an OD_{600} value of 1.0, followed by incubation at 37 °C.

2.2. Oligonucleotides, plasmids, disruption of target genes

The sequences of oligonucleotides used in this study are shown in Table 2. A polymerase chain reaction (PCR)-based gene disruption method was utilized to construct the BWP17, *VMA4*, and *VMA10* heterozygous and homozygous deletion strains (Walther and Wendland, 2008).

To generate CJK126, the *CaURA3* gene was amplified from SC5314 genomic DNA by PCR with specific primers (JK12129 and JK12130). This amplified CaURA3 gene was transformed into to BWP17, generating the *URA3* reconstituted strain.

To generate the *VMA4* deletion mutant (CJK129), primers (JK0775 and JK0776) containing 20 base pairs homologous to *HIS1* and 100 base pairs homologous to *VMA4* were used to amplify a *HIS1* marker cassette (Wilson et al., 2000). This cassette was transformed into BWP17, generating the *VMA4* single deletion mutant. To delete another *VMA4* allele, transformation was carried out with the *ARG4* marker cassette and amplified by specific primers (JK12012 and JK12103).

To generate the *VMA10* deletion mutant (CJK133), oligonucleotides were designed to amplify the *HIS1* or *ARG4* cassette. These cassettes were amplified by specific primers (JK0874, JK0875, JK0876, and JK0877) using SC5314 genomic DNA as a template.

The PCR conditions were as follows: 94 °C for 5 min followed by 33 cycles at 94 °C for 30 s, 50 °C for 30 s, 72 °C for 1 min, and polymerization at 72 °C for 10 min. In general, 100 μl of the PCR products of each deletion cassette was subsequently added to a single transformation using a general lithium acetate (LiAc) method. The deletions were confirmed by PCR using genomic DNA of each strain with specific primers.

Vma4-GFP and Vma10-GFP strains were created by transforming BWP17 with their respective fusion cassettes. pMG1646 was used as the template for the fusion cassette. The primer sequence of the C-terminal GFP tagging cassette is shown in Table 2.

For the complementation assay, *CaVMA4* or *CaVMA10* was digested with XhoI and NotI. These inserts were cloned into pNH4 (Park and Choi, 2002). pNH4-*CaVMA4* was transformed into the BY4741*vma4Δ* strain and pNH4-*CaVMA10* was transformed into the BY4741*vma10Δ* strain.

To generate the *vma4ΔR* or *vma10ΔR* strain, the *pBS-ADH1pomoter-VMA4-URA3-ADH1*, *pBS-ADH1pomoter-VMA10-URA3-ADH1* plasmid was constructed. The *ADH1* promoter (- 1000 nt to 0 nt) or *ADH1* fragment (+323 nt to +1053 nt) for homologous recombination was amplified from genomic DNA of SC5314 strain. This *ADH1* insert was cloned into the pBluescript SK + using XbaI and NotI, and promoter of *ADH1* was cloned into the same plasmid using KpnI and ApaI, resulting in the *pBS-ADH1promoter-ADH1* plasmid. The *URA3* selection marker was amplified from genomic DNA of SC5314 strain. *URA3* was cloned into *pBS-ADH1promoter-ADH1* using BamHI and SpeI, resulting in the generation of *pBS-*

Table 1
Candida albicans strains used in this study.

Strain	Relevant genotype	Source
SC5314	Clinical isolate from London Mycological Reference Laboratory	Fonzi and Irwin (1993)
BWP17	*ura3::imm434/ura3::imm434 his1::hisG/his1::hisG arg4::hisG/arg4::hisG*	Wilson et al. (1999)
CJK126	*As BWP17 except ura3::imm434/ura3::imm434::URA3*	This study
CJK127	*As CJK126 except vma4::HIS1/VMA4*	This study
CJK128	*As CJK126 except VMA4/vma4::ARG4*	This study
CJK129	*As CJK126 except vma4::HIS1/vma4::ARG4*	This study
CJK130	*As CJK129 except ADH1/adh1::VMA4-URA3*	This study
CJK131	*As CJK126 except vma10::HIS1/VMA10*	This study
CJK132	*As CJK126 except VMA10/vma10::ARG4*	This study
CJK133	*As CJK126 except vma10::HIS1/vma10::ARG4*	This study
CJK134	*As CJK133 except ADH1/adh1::VMA10-URA3*	This study
CJK135	*As CJK128 except vma4::VMA4-GFP-HIS1/vma4::ARG4*	This study
CJK136	*As CJK132 except vma10::VMA10-GFP-HIS1/vma10::ARG4*	This study
CJK137	*As CJK126 except ADH1/adh1::TetO-UME6-NAT*	This study
CJK138	*As CJK129 except ADH1/adh1::TetO-UME6-NAT*	This study
CJK139	*As CJK133 except ADH1/adh1::TetO-UME6-NAT*	This study

Table 2
Oligonucleotides used in this study.

Primer	Sequence (5′−3′)	Source
JK0775	ATGGCTTTATCAGACGAACAGGTATGTTAGATATTAGATTGAATATGTGTTTTAGACCTTGTGATAATGTTACTAACCGCTTTGTCTAGGTTAAATCGGA TGGTAGTGAAAACCCCGG	*VMA4-HIS1* deletion cassette (forward)
JK0776	TAAGTTACAAATTTTCAAATTATATATAAAAAAAAAAATACTAATAATATTTGATGTTGAGAGGTAATACTAATAAAGGAAACACTCATCTTATATCAA GAATGCCTATTGACTTTAAAGGTG	*VMA4-HIS1* deletion cassette (reverse)
JK12102	ACTCTCCAAAATGCAAGCCTTCATTGAGAAGGAAGCTAAGGAGAAGGCTAAGGAAATCAAATTGAAAGCCGACGAAGAATATGAAATTGAAAAGGC ATCCCCCCTTTAGTAAGATTTTTCA	*VMA4-ARG4* deletion cassette (forward)
JK12103	TTAATCAAAGAATTTTCTAGTGGTTGAAGGTCCAAATAATTCTAATCTAATAGCTGGCAAAGCTTCTTCGGATAAGATCTTCAATCTTTCTTCTAAAGTT ATGGTTAGGATATTATTAGG	*VMA4-ARG4* deletion cassette (reverse)
JK0874	CCGAAACTCTCAAAATGTTCACTGATAAAGCTTAACACACCAACACTCTCAATCAGAAGTGCTTAACAAGTGCAATCCCCGTCCCCAATTATTATCCAT ATGGTAGTGAAAACCCCGG	*VMA10-HIS1* deletion cassette (forward)
JK0875	TTATTGAGATGCATTTATGTGTAAAGTTGGTGTTGGCTTGACAGTAGCGTCAACTAACAATTTAACAACTGCACTCTTTTTCTTTTCAAAAGTGGATTTG AATGCCTATTGACTTTAAAGGTGT	*VMA10-HIS1* deletion cassette (reverse)
JK0876	AAGATTGAATGATAGAAAACTATACATATTTGATCAATATACACGACTAATATATTTACATTTGACACGACCCAATTTCTATTTTTCCAACATTGTCGCA CCCCTTTAGTAAGATTTT	*VMA10-ARG4* deletion cassette (forward)
JK0877	ATGAATTACTATCAATTATTTTTTTTTTCTAAACATAACTATAATTGTAACCATTTAAATACATTTATTGTAATTGTTGGAGATCGTCTTGTTTGCCTGGC ATATTTGCAAGTATGGTTAG	*VMA10-ARG4* deletion cassette (reverse)
JK1067	TTTTGGGCCCTGGCTTTATCAGACGAACAG	*VMA4* cloning into pBS-SK$^+$ (forward)
JK1068	TTTCTGCAGTTAATCAAAGAATTTTCTAGTGGTT	*VMA4* cloning into pBS-SK$^+$ (reverse)
JK1069	TTTTGGGCCCATGTCATCTGGTATCCAAT	*VMA10* cloning into pBS-SK$^+$ (forward)
JK1070	TTTTAAGCTTTTATTGAGATGCATTTATGTGTAAA	*VMA10* cloning into pBS-SK$^+$ (reverse)
JK1047	TTTTGGATCCTTCAGAACAAAATCCATTTCA	*URA3* cloning into pBS-SK$^+$ (forward)
JK1003	TTTTATCAGTTTATAATGCATCACGATT	*URA3* cloning into pBS-SK$^+$ (reverse)
JK1274	ATGGCTTTATCAGACGAACAG	*VMA4* deletion, reintegration confirmation (forward)
JK12101	TTAATCAAAGAATTTTCTAGTGGTT	*VMA4* deletion, reintegration confirmation (reverse)
JK1273	TTATTTACTGGTGTCCAAGACGTATC	*VMA4-URA3*, *VMA10-URA3* reintegration confirmation (reverse)
JK09121	ATGTCATCTGGTATCCAAT	*VMA10* deletion, reintegration confirmation (forward)
JK09122	TTATTGAGATGCATTTATGTGTAAA	*VMA10* deletion, reintegration confirmation (reverse)
JK1517	ACTTTAGAAGAAAGATTGAAGATCTTATCCGAAGAAGCTTTGCCAGCTATTAGATTAGAATTATTTGGACCTTCAACCACTAGAAAATTCTTTGAT GGT GGT GGT TCT AAA GGT GAA GAA TTA TT	VMA4-GFP tagging cassette (Forward)
JK1518	TTA CAA ATT TTC AAA TTA TAT ATA AAA AAA AAA ATA CTA ATA ATA TTT GAT GTT GAG AGG TAA TAC TAA TAA AGG AAA CAC TCA TCT TAT ATC AAG GAA TTC CGG AAT ATT TAT GAG AAA C	VMA4-GFP tagging cassette (reverse)
JK1519	AAATCCACTTTTGAAAAGAAAAAGAGTGCAGTTGTTAAATTGTTAGTTGACGCTACTGTCAAGCCAACACCAACTTTACACATAAATGCATCTCAAGGT GGTGGTTCTAAAGGTGAAGAATTATT	VMA10-GFP tagging strain cassette (Forward)
JK1520	ACT ATC AAT TAT TTT TTT TTT CTA AAC ATA ACT ATA ATT GTA ACC ATT TAA ATA CAT TTA TTG TAA TTG TTG GAG ATC GTC TTG TTT GCC TGG CAT GAATTCCGGAATATTTATGAGAAAC	VMA10-GFP tagging strain cassette (reverse)
VMA4-F	ATGTTGCCAAAGAAGCCATAAC	Quantitative PCR
VMA4-R	ACCACCAGCGATATCTTTAGC	Quantitative PCR
VMA10-F	ACAAGATGCTCAAGCTGAAATTG	Quantitative PCR
VMA10-R	AGCATCAGCTTCTTTATCGATCT	Quantitative PCR
UME6-F	CATTCAATCCTACTCGTCCACC	Quantitative PCR
UME6-R	CAACTCCAGATCCAGTAGCAG	Quantitative PCR
HGC1-F	ATATACACCAGGTCGAAGC	Quantitative PCR
HGC-R	AGAAACAGCACGAGAACCAG	Quantitative PCR
ACT1-F	TCAGACCAGCTGATTTAGGTTTG	Quantitative PCR
ACT1-R	GTGAACAATGGATGGACCAG	Quantitative PCR

Underlines indicate the sequence of the enzyme site.

ADH1promoter-URA3-ADH1. *VMA4* or *VMA10* ORF was amplified from genomic DNA of SC5314 strain and was cloned into *pBS-ADH1promoter-URA3-ADH*, resulting in *pBS-ADH1promoter-VMA4-URA3-ADH1*, *pBS-ADH1promoter-VMA4-URA3-ADH1* plasmid. These plasmids were restricted to KpnI and NotI to generate linear cassette DNA. This linear cassette DNA was transformed into *vma4Δ* or *vma10Δ* strains.

2.3. Identification of differentially expressed proteomes in yeast and hyphae cells

Cells were harvested by centrifugation and washed with distilled water for 2D-PAGE. The cell pellet was resuspended in 0.4 ml of lysis buffer [50 mM Tris–HCl (pH 7.5), 100 mM NaCl, 0.1 % Triton X-100, 1 μg/ml of DNase, and 1 μg/ml of RNase], supplemented with protease inhibitors (1 mM PMSF, 1 μg/ml of aprotinin, pepstatin A, and leupeptin). Cell disruption was performed with glass beads as described previously (Joo et al., 2009). The protein lysates (300 μg) were subjected to first dimensional separation carried out on an Ettan-IPGphor Isoelectric focusing unit (Amersham Bioscience; Piscataway, NJ, USA) at 20 °C. Additionally, an Immoliline pH 4–7 gradient strip (Amersham Bioscience) was used. 2D separation based on molecular weight was carried out by 12.5 % PAGE, followed by silver staining of the gels. Gel spots of interest were selected, such as those showing an increase or decrease of more than 1.5-fold. Silver-stained protein spots were excised and stain-stripped in 100 mM sodium thiosulfate and 30 mM potassium ferricyanide. Proteolytic peptides were recovered from the gel by in-gel digestion using 12 ng/μl sequencing-grade trypsin (Promega; Madison, WI, USA) in 25 mM ammonium bicarbonate. Mass spectrometric (MS) analyses were performed using an AB 4700 Proteomics Analyzer (Applied Biosystems; Foster City, CA, USA) in both the MS and MS/MS modes. The mass spectrometer was set to acquire positive ion MS survey scans over a mass range of 700–3500 Da. Once the MS survey scans were completed, the data were processed to generate a list of precursor ions for investigation by MS/MS. The instrument was equipped with an Nd: YAG laser (PowerChip) operating at 200 Hz and controlled with Applied Biosystems Explorer (ver. 1.1) software. The mass resolution of the instrument was 15,000 and 4000 in MS and MS/MS modes, respectively. The mass accuracy in MS mode was roughly ±30 ppm, whereas in MS/MS mode, it was ±100 ppm. The MS/MS was performed with air as the collision gas at a pressure of 1.4×10^{-6} Torr. Protein identification was performed by an MS/MS ion search (mass tolerance for precursor ion, 150 ppm; fragment ion, 0.5 Da), based on the time of flight (TOF)/TOF tandem MS data from at least two peptides to search the Swiss-Prot protein database (release 46.3, 176,469 sequences) using Mascot (ver. 1.9, MatrixScience; Cambridge, UK). Searches were performed allowing a fixed modification of carbamidomethylation at cysteines and a maximum of one missed trypsin cleavage. All automatic data analyses and database searching were performed with the GPS Explorer software (ver. 3.5, Applied Biosystems). Protein scores >81 were considered significant ($p \leq 0.05$).

2.4. Test of pH and metal ion-sensitive growth

Each strain was grown to a stationary phase in YPD medium at 30 °C. Dilution was performed to an OD_{600} of 1.0, followed by streaking on a plate supplemented with uridine (50 μg/ml) and the appropriate metal ions. A solid Sabouraud medium [2 % glucose, 1 % peptone (casein), 2 % agar, and 100 mM Trisma base] was used to examine the pH-dependent growth (Poltermann et al., 2005). The pH of the plate was adjusted to 4.0 and 8.0, with 1 M citric acid solution.

2.5. Cell staining with quinacrine and FM4-64

To investigate vacuolar acidification, quinacrine was used as described previously (Shao and Forgac, 2004). Exponentially growing cells (1.0×10^7) were harvested and resuspended in 500 μl of staining buffer (YPD harboring 50 mM Na_2HPO_4, pH 7.6). Then, 2.5 μl of a quinacrine solution [25 mg/ml of quinacrine (Sigma; St. Louis, MO, USA) in YPD containing 100 mM Tris-citrate (pH 7.6)] was added. After 10 min of incubation with shaking at 30 °C, the cells were sedimented by centrifugation and washed three times with 1 ml of washing buffer (2 % dextrose, 50 mM Na_2HPO_4, pH 7.6). The cell pellet was resuspended with 500 μl of washing buffer. Five microliters of the cell suspension was then applied to a microscope slide and visualized with a fluorescence microscope (Zeiss Oberkochen; Germany). Quantitation of quinacrine accumulation was measured by ZEN lite 2011 software. The vacuolar pH was quantified with BCECF-AM (Invitrogen; Carlsbad, CA, USA) as described previously (Raines et al., 2013). To examine vacuole fusion, FM4-64 (Invitrogen; Carlsbad, CA, USA) staining was carried out, as described previously, with some modifications (Vida and Emr, 1995). Approximately 1.0×10^7 cells were collected and washed twice with 1 ml of phosphate buffered saline (PBS). The cell pellet was resuspended in 500 μl PBS containing 2 μM of FM 4–64 and was labeled for 1 h with shaking. Cells were harvested and washed four times with 1 ml PBS. The pellets were finally resuspended in 500 μl of PBS, and 5 μl of the suspended cells was examined with a fluorescence microscope (Zeiss).

2.6. Real time PCR

Pre-cultured *C. albicans* cells were diluted in 10 ml of fresh YPD at 30 °C to induce yeast growth or in fresh YPD supplemented with 10 % serum at 37 °C to induce the yeast-to-hyphae transition. The total RNA samples were isolated from each cell culture using general hot-phenol methods (Schmitt et al., 1990). The total RNA was measured by a Nanodrop 1000 Spectrophotometer (Thermo Scientific; Rockford, IL, USA), and was reverse transcribed into cDNAs using oligo-d(T) and AMV reverse transcriptase (Promega). Real-time PCR was performed with *VMA4*-, *VMA10*-, *UME6*-, *HGC1*-, and *ACT1*-specific primers using a Lightcycler 480 (Roche; Manheim, Germany).

2.7. V-ATPase activity and proton transport assay

The Ficoll density gradient centrifugation method was used to purify the vacuolar membranes (Owegi et al., 2006). ATPase activity was measured spectrophotometrically using an ATPase assay Kit (BioAssay Systems, USA) and ATP hydrolysis was quantified at 620 nm on a plate reader. Each reaction contained 5 μg of a vacuolar membrane vesicle. Proton transport of purified vacuolar vesicles (15 μg) was measured via quenching of 1 μM 9-amino-6-chloro-2-methoxyacridine (ACMA) upon the addition of 0.5 mM ATP–1 mM $MgSO_4$ (MgATP), as described previously (Chan et al., 2012) (Rane et al., 2013).

2.8. Virulence test using a mouse model

Overnight-cultured *C. albicans* strains were pelleted and washed three times with 1 ml sterile PBS. Approximately 1.0×10^6 cells were resuspended in 200 μl PBS and injected into 5-week-old BALB/c (male) mice (n = 10 each) via the lateral tail vein. The mice were monitored for 1 m and Kaplan–Meier survival curves were plotted.

2.9. Antifungal test

Overnight cultured each strain was diluted with PBS and spotted onto YPD supplemented with fluconazole (4 μg/ml), amphotericin

B (2 μg/ml), or terbinafine (4 μg/ml). YPD plates without drugs were used as a control. The plates were incubated at 30 °C for 1 d.

Overnight-cultured SC5314 cells were pelleted and washed with 1 ml sterile PBS. Approximately 1.0×10^6 cells were resuspended in 100 μl PBS and smeared on a plate supplemented with vehicle (DMSO), 0.5 μM bafilomycin A1, or 1 μM concanamycin A. An autoclaved disk containing 2.5 μM fluconazole was patched on the same plates. The plates were incubated at 30 °C for 1 d.

2.10. Ethics statement

This study was performed according to the guidelines of the Institutional Animal Care and Use Committee of Korea University. All animal experiments were approved by the Institutional Animal Care and Use Committee of Korea University. The Permit Number is KUIACUC-2009-51. All mice used in the experiments were sacrificed with minimum suffering.

3. Results

3.1. Identification of Vma4 as a putative hyphal-specific protein in C. albicans

The ability of *C. albicans* to undergo morphological transition is believed to be critical for its virulence (Calderone and Fonzi, 2001; Lo et al., 1997). To identify the hyphal-specific proteins of *C. albicans*, the wild-type *C. albicans* (SC5314) strain was cultivated to undergo yeast growth in YPD medium at 30 °C for 4 h or was cultured to undergo hyphae growth in YPD medium in the presence of serum at 37 °C for 4 h. Equal amount of protein lysates (300 μg) were prepared from yeast and hyphae cells. Subsequently, sets of proteomic analyses, including 2D-PAGE, in-gel digestion, and MS/MS, were performed to identify the proteins that significantly increased or decreased during morphological conversion. These analyses identified 131 proteins whose expression levels were changed by more than 1.5-fold during hyphal morphogenesis. Eighty-three proteins were upregulated in expression whereas 48 proteins were downregulated (Table S1). Some of them had previously been identified in the total cytoplasmic extract 2D-DIGE analysis. Rdi1 which is a Rho protein GDP dissociation inhibitor involved in actin filament organization was increased its amount in hyphae cells (Monteoliva et al., 2011). One of the proteins increased during hyphae formation found in our 2D-DIGE analysis is Bmh1. Bmh1 is a 14-3-3 family protein which is involved in RAS protein signal transduction and in hyphal growth (Cognetti et al., 2002). Atp2 was found in our proteomic analysis. It is well known as an F_1 beta subunit of F_1F_0 ATPase complex. Atp2 was also found to be a protein whose expression decreased during the morphological changes. It was revealed that Atp2 is required for *C. albicans* pathogenicity and operates by affecting metabolic flexibility in carbon consumption (Li et al., 2018).

Among these proteins, we first focused on Vma4, which showed increase (by 3.6-fold) in the transition from the yeast form to the hyphae form (Fig. 1A). Vma10 is known to form a tight heterodimer with Vma4 in the stalk region of V-ATPase. *Ohira* et al. found that not only the E subunit (Vma4) is dependent on the presence of subunit G (Vma10) for stability, it is also dependent on the correct ratio of the E and G subunits (Ohira et al., 2006). Therefore, the expression of Vma10 is also expected to increase similarly to Vma4 in the hyphae growth condition (Forgac, 2007; Ohira et al., 2006; Oot and Wilkens, 2010). To confirm the intracellular localization of these proteins and the amount of expression of each protein under various hyphal growing conditions, we generated BWP17 strains endogenously expressing Vma4-GFP- and Vma10-GFP proteins. The intracellular localization of Vma4 and Vma10 were confirmed by fluorescence microscopy in the strains generated. As expected, Vma4 and Vma10 were actually present in the vacuole membrane. Expression of Vma4 and Vma10 were increased by 2.7-fold and 1.8-fold, respectively, during hyphal morphogenesis in various conditions such as the presence of serum, temperature change, spider medium, and pH change (Fig. 1B, C, Fig. S1B). To check the transcription level of *VMA4* and *VMA10* during hyphal growth, qPCR was performed (Fig. 1D and E). Transcription of *VMA4* and *VMA10* was also increased during hyphal growth. Vma4 and Vma10 are already known as the E and G subunits of the V-ATPase V_1 domain, respectively, in *Saccharomyces cerevisiae*. The putative ORF of *C. albicans VMA4* encodes a polypeptide of 212 amino acids that is 56 % identical to *S. cerevisiae* Vma4, while *CaVMA10* encodes 114 amino acids that are 50 % identical to ScVma10 (Fig. S2). We also sought to confirm that CaVma4 and CaVma10 are orthologs of *S. cerevisiae*; CaVma4 and CaVma10 were expressed in *vma4* and *vma10* deletion strains of *S. cerevisiae* for a complementation assay (Fig. S3). In this study, the growth was recovered in complementation strains. Therefore, CaVma4 and CaVma10 were confirmed to be orthologs of ScVma4 and ScVma10, respectively.

To determine the roles of Vma4 and Vma10 during morphogenesis and pathogenesis, two alleles of both genes were serially deleted by PCR-based gene disruption on a BWP17 background. Reconstituted strains were also generated in which VMA4 or VMA10 were reintroduced into *vma4Δ* or *vma10Δ* strains (Fig. S4).

3.2. Vma4 and Vma10 are required for resistance to cellular stressors

Ion homeostasis is important for toxic metal detoxification (Klionsky et al., 1990). During this process, toxic ions are sequestered via a proton gradient generated by V-ATPase (Beyenbach and Wieczorek, 2006). To determine the functionality of metal ion detoxification in *vma4Δ* and *vma10Δ* mutants, each strain was plated onto YPD agar, then supplemented with increasing concentrations of various metal salts such as $ZnCl_2$, $CoCl_2$, $CuSO_4$, $MnCl_2$, and $NiSO_4$. It was found that both deletion mutants showed hypersensitive growth under high concentrations of all metal ions, whereas the wild-type, heterozygote mutants, and reconstituted strains grew normally (Fig. 2A). This result suggested that Vma4 and Vma10 are involved in detoxifying most metal ions *in vivo*. The growth sensitivity to pH for *vma4Δ* and *vma10Δ* strains was also investigated. These mutants showed defective growth at alkaline pH values (7.5 and 8) (Fig. 2B and C). Furthermore, *vma4Δ* and *vma10Δ* mutants were unable to grow in the presence of glycerol as a non-fermentable carbon source (Fig. 2C). Based on these data, it was found that *vma4Δ* or *vma10Δ* in *C. albicans* represents *vma*-phenotype.

3.3. vma4Δ and vma10Δ mutants are defective in vacuolar acidification and vacuole morphology

To demonstrate that the *vma4Δ* and *vma10Δ* mutants inhibit vacuolar acidification by V-ATPase, vacuolar acidification was investigated using quinacrine, which is an acidophilic fluorescent dye. This dye emits fluorescence in the vacuole because of its low luminal pH. Neither *vma4Δ* nor *vma10Δ* strains showed any positive fluorescence signal in the cytosol (Fig. 3A and B). Wild-type and reconstituted strains did have clear positive fluorescent spots, indicating that *vma4Δ* and *vma10Δ* strains do not have any acidic endosomal compartments, suggesting a functional defect in the V-ATPase complex. Furthermore, there were no clear and positive fluorescent spots detected in cells treated with concanamycin A, which is a V-ATPase specific inhibitor (Fig. S5). Also, vacuolar pH was measured using BCECF, which is a pH-sensitive fluorophore

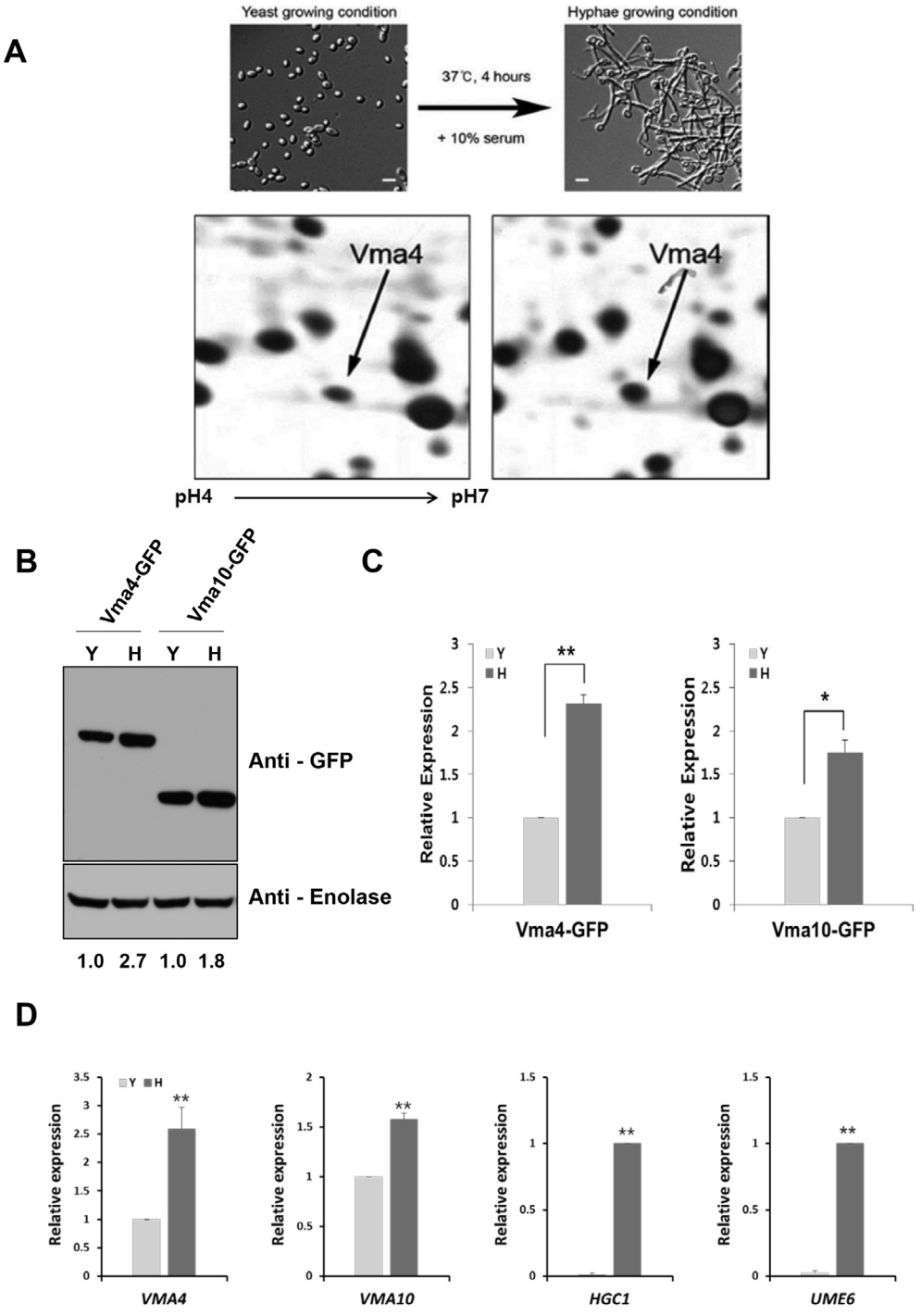

Fig. 1. Identification of differentially regulated proteins between yeast and hyphae-growing cells in *Candida albicans*. (A) The wild-type strain (SC5314) was grown to late log phase and re-cultured under yeast- (30 °C, YPD) and hyphae-growing conditions (37 °C, YPD containing 10 % serum). Protein lysates were generated after 4 h of incubation. Equal amount of protein lysates (300 μg) in each conditions was subjected to two-dimensional (2D) polyacrylamide gel electrophoresis, followed by matrix-assisted laser desorption/ionization-time-of-flight analysis to identify the differentially expressed proteins. Images of silver-stained 2D-gels are shown in the lower panel. Cell images were taken using differential interference phase contrast microscopy (Zeiss × 200). All scale bars represent 10 μm. (B) VMA4-GFP or VMA10-GFP tagged strains were generated and grown in the same conditions as in (A). Protein lysates were generated with lysis buffer (50 mM Tris-Cl (pH 7.5), 150 mM NaCl, 0.1 % NP-40). Expression of Vma4 or Vma10 was analyzed by Western blot using an anti-GFP antibody. (C) Each experiment was performed for 3 separate cultures and the expression of each protein was normalized to that of enolase (Western blot) and quantified using Image J 1.48 software. Vacuolar protein expressions are shown as the average ± Standard Deviation (SD). *P < 0.01. (D) The total RNA was measured with a Nanodrop 1000 spectrophotometer, and was reverse transcribed into cDNAs using oligo-d(T). Then, cDNA was amplified with indicated genes. Real time polymerase chain reaction was performed with *VMA4*, *VMA10*, *UME6*, *HGC1*, and *ACT1* specific primers. Expressions of each gene were normalized with actin transcript level. The induction rate of each gene in the indicated condition is shown as the average ± SD for n = 3 separate RNA purifications (Y = Yeast, H = Hyphae).

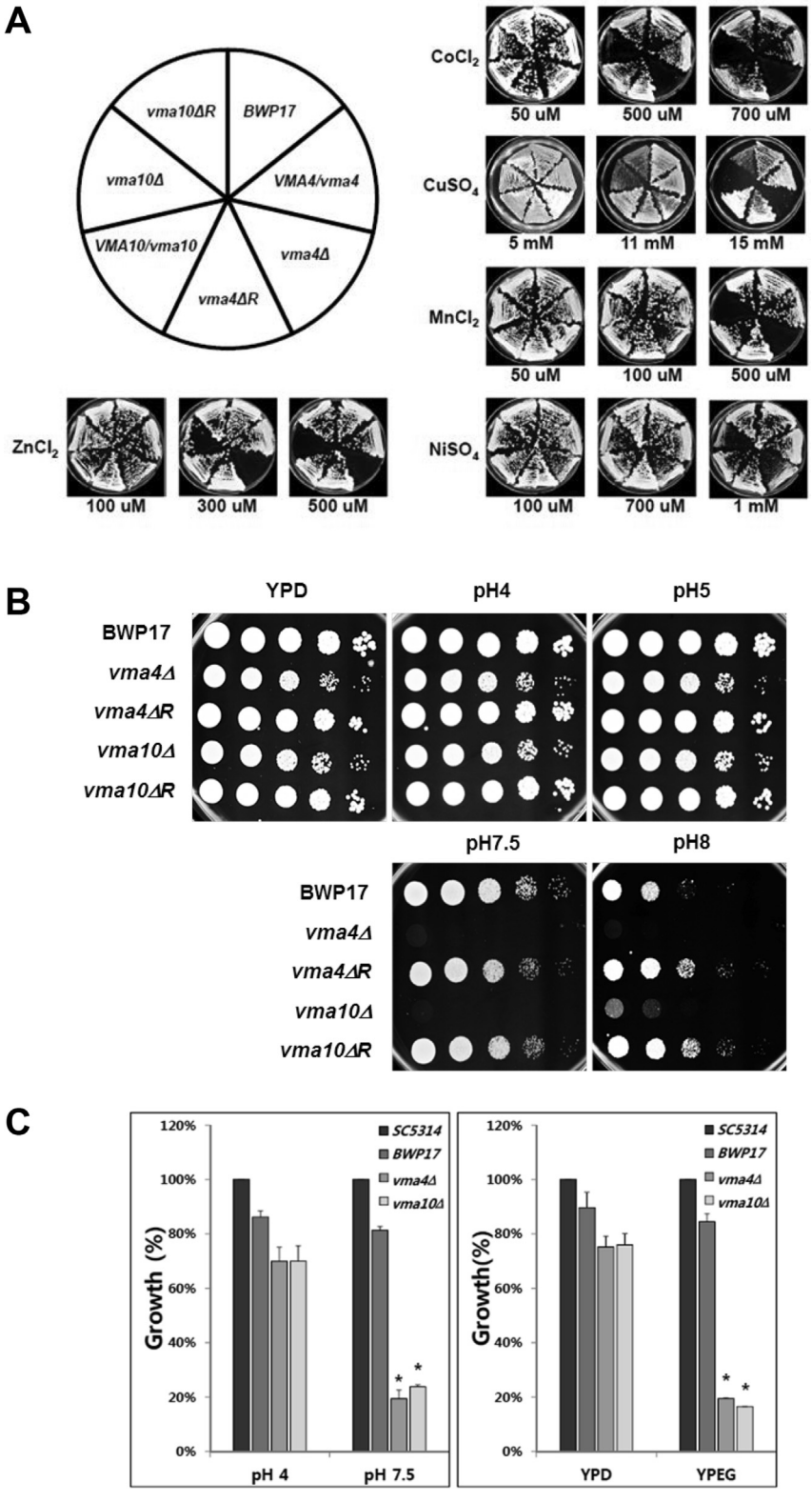

Fig. 2. vma4Δ and vma10Δ mutants showed hypersensitivity to cellular stressors. (A) Disruption of *VMA4* or *VMA10* caused defects in metal ion detoxification. Wild-type (BWP17), heterozygote, *vma4Δ*, *vma10Δ*, *vma4ΔR*, and *vma10ΔR* strains were plated onto YPD agar supplemented with the indicated concentrations of metal salts. Plate images were taken after 3 d of incubation at 30 °C. (B) Each strain, grown in YPD for 16 h, was diluted with PBS and spotted onto YPD, with SC used as a control and SC agar media at pH values of 4, 5, 7.5 and 8. Cell densities of each spot were 1×10^5, 1×10^4, 1×10^3, 1×10^2, and 1×10^1 in each plate from left to right. Strains are indicated to the left of the plate figure. The plate images were scanned after 4 d of incubation at 30 °C. (C) The same strains in (B) were inoculated in the indicated medium at an OD_{600} value of 0.1 at 30 °C for 18 h and growth was measured with a spectrophotometer at OD_{600}. SC5314 strain was considered as 100 % growth. This experiment was performed for 3 separate cultures, and the results were expressed as a percentage of the SC5314 control. *$p < 0.001$ versus SC5314.

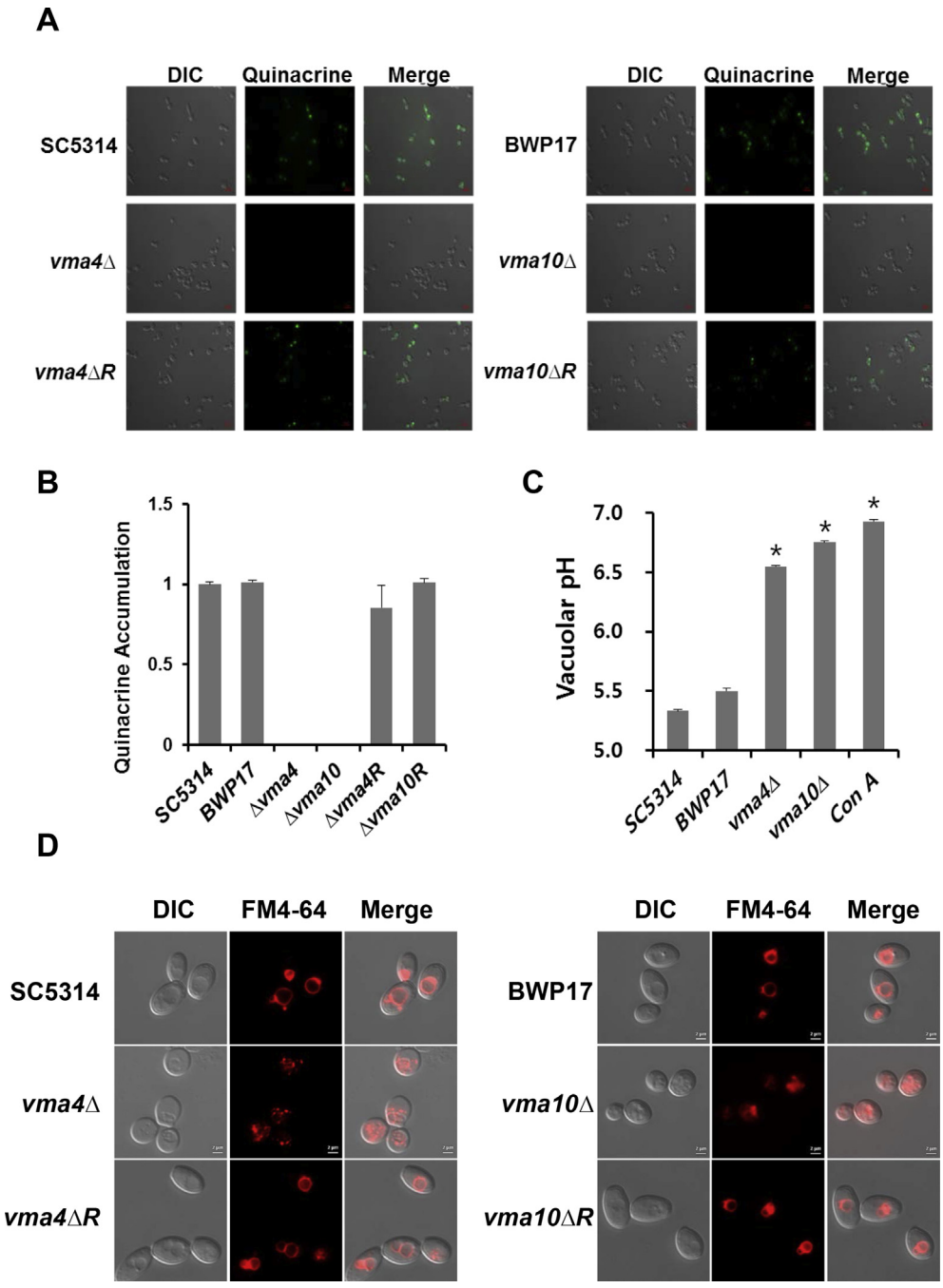

Fig. 3. Vacuole acidification is defective in *vma4Δ* and *vma10Δ* mutants. (A) Cells (SC5314, BWP17, *vma4Δ*, *vma10Δ*, *vma4ΔR*, and *vma10ΔR*) were stained with quinacrine, and images of their morphology and fluorescence signals were obtained using differential interference microscope and fluorescence microscopy, respectively (Zeiss, × 630). (B) Quinacrine accumulation in each strain was measured by Zen lite 2011 software. (C) Vacuolar pH was measured using the ratio metric fluorescent dye BCECF-AM, and calculated as described previously. (D) Cells of each strain were labeled for 1 h with FM4-64. Cell images were detected using the same microscopy method as in (A). The vacuolar pH values and quinacrine accumulations are shown as the average ± SD. For n = 3 separate experiments, the vacuolar pH values of all strains are indicated. *p < 0.001 versus BWP17.

that accumulates in the fungal vacuole. The vacuolar pHs in wild-type strains (SC5314 and BWP17) were 5.332 ± 0.010 and 5.500 ± 0.025, respectively. However, the vacuolar pH of concanamycin A-treated wild-type cells was increased to 6.928 ± 0.012. The *vma4Δ* and *vma10Δ* strains also showed increased pH to 6.549 ± 0.005 and 6.752 ± 0.01, respectively, indicating vacuolar alkalization (Fig. 3C). Next, vacuolar membrane morphology was examined using the fluorescent dye FM4-64. This lipophilic dye first embeds itself in the plasma membrane and later is enriched in vacuolar membranes (Vida and Emr, 1995). As shown in Fig. 3D, most of the fluorescence signals were detected within a clear ring-like structure in the wild-type and reconstituted cells after 1 h of labeling. However, *vma4Δ* and *vma10Δ* mutants showed numerous tiny fragments throughout the cytosol. These fragments were also detected in concanamycin A-treated cells (Fig. S6). These results suggested that Vma4 and Vma10 are involved in vacuole membrane morphology. Protease and lipase secretion is known to be involved in the pathogenesis of *C. albicans* by supporting invasion into the host tissue. To confirm this hypothesis, a bovine serum albumin (BSA) hydrolysis assay was performed. As hypothesized,

the activity of the secreted protease was defective in both null mutants (Fig. S7). Plaque halos, which confirm BSA hydrolysis by a protease, were not detected in either deletion strain. Taken together, it is concluded that Vma4 and Vma10, as subunits of peripheral stalk region in V-ATPase complex, are required for vacuolar acidification, proper morphology of the vacuole membrane, and protease secretion in *C. albicans*.

3.4. *Vma4 and Vma10 are required for V-ATPase activity*

To establish the effect of Vma4 and Vma10 on V-ATPase activity, such as ATP hydrolysis and proton transport, we purified the vacuole from BWP17 cultured with or without concanamycin A, *vma4Δ*, and *vma10Δ* cells grown in YPD. ATP hydrolysis was measured spectrophotometrically using an enzymatic assay, and proton transport activity was measured fluorometrically using 9-amino-6-chloro-2-methoxyacridine (ACMA). As expected, ATP hydrolysis activity was decreased in concanamycin A treated wild type, *vma4Δ* and *vma10Δ* cells, compared to concanamycin A untreated wild-type cells (Fig. 4A). Proton transport activity was also reduced in concanamycin A treated wild type, *vma4Δ* and *vma10Δ* cells more than in concanamycin A untreated wild-type cells (Fig. 4B). These results show that Vma4 and Vma10 are required for ATP hydrolysis activity and proton transport activity in the V-ATPase of *C. albicans*.

3.5. vma4Δ *and* vma10Δ *mutants are defective in hyphal growth*

To examine whether the *vma4Δ* and *vma10Δ* mutants exhibited altered morphological conversion, hyphal growth was induced in each strain with various conditions. Under these conditions, wild-type and reconstituted cells changed their morphology from yeast to filamentous forms. However, the *vma4Δ* and *vma10Δ* cells grew mostly in yeast forms (Fig. 5A). To further investigate the functional relevance of Vma4 and Vma10, hyphal morphogenesis was induced on solid agar (Fig. S8). Consistent with the previous results in liquid media, *vma4Δ* and *vma10Δ* strains showed defective hyphal formation on YPD-serum plates. During morphological transition, *C. albicans* changes the expression patterns of many genes (Liu, 2001). A novel hyphal-specific transcriptional regulator of *C. albicans*, Ume6, is induced in response to multiple environmental cues and is specifically important for hyphal extension (Banerjee et al., 2008). It is also known that morphological transition occur without the hyphae growth stimulus according to the degree of *UME6* expression. To characterize pathways and regulators of hyphal growth in *vma4Δ* and *vma10Δ* strains, TetO-*UME6* BWP17, TetO-*UME6 vma4Δ*, and TetO-*UME6 vma10*Δ strains were generated. As seen in Fig. 5B, when *UME6* was induced by doxycycline in yeast growing conditions, *vma4* or *vma10* deletion strains did not change their morphology, but wild type strains did. This suggests either that V-ATPase functions downstream of Ume6, or that V-ATPase functions during filamentous growth involve independent mechanisms.

3.6. *Inhibitors of V-ATPase reduce the rate of morphological transition*

Genetic analyses shown in section 3.5 revealed that Vma4 and Vma10 are involved in hyphal morphogenesis. However, results from the gene deletion experiments present the possibility of side effects caused by the gene deletion itself. To exclude this possibility, bafilomycin A1, a V-ATPase inhibitor, was utilized. SC5314, which is a clinically isolated strain, was inoculated into the media with or without serum and bafilomycin A1 (Fig. 6A). The formation and emergence of germ tubes were clearly observed in serum-treated cells. However, true hyphae formation was partially blocked by bafilomycin A1. Under this condition, some cells still existed in a yeast form while others showed pseudohyphal growth. Furthermore, the germ tube length of bafilomycin A1 treated cells in YPD-serum media was significantly shorter than that of untreated cells. Quantitative analysis of the number of each cell (yeast, pseudohyphae, and true hyphae cells) can be seen in Fig. 6B. Concanamycin A is also a specific inhibitor of V-ATPase. SC5314 was incubated in media containing serum and concanamycin A. Cells treated with concanamycin A did not induce filamentation (Fig. S6). These results showed that the activity of the V-ATPase complex including Vma4 and Vma10 in *C. albicans* is critical for hyphal morphogenesis, including germ tube emergence and hyphal tip elongation.

3.7. *Vma4 and Vma10 are essential for* C. albicans *pathogenesis*

In general, non-filamentous *C. albicans* strains are thought to be avirulent (Lo et al., 1997). Recently, it was confirmed by other

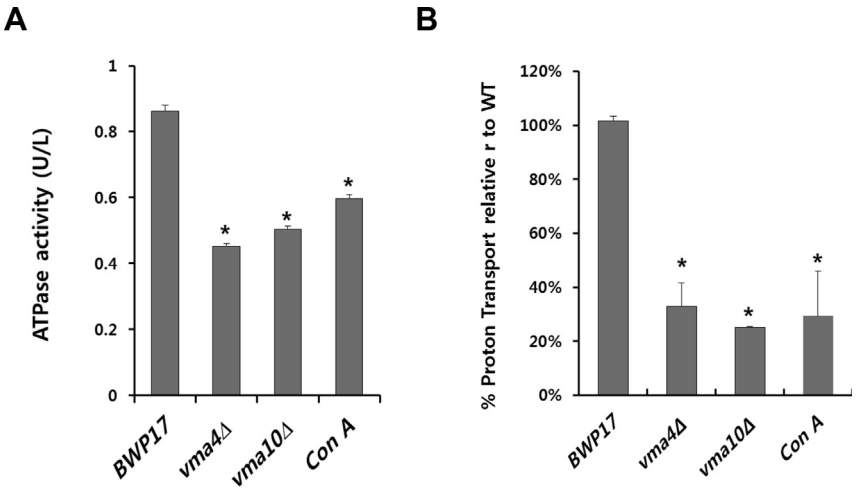

Fig. 4. VMA4 and VMA10 are required for V-ATPase activity. (A) Vacuoles were purified by Ficoll density gradient centrifugation in indicated strains or concanamycin A treated wild type cells. ATPase-specific activity was measured in purified vacuolar vesicles using a spectrophotometric enzyme assay. (B) Proton transport of purified vacuolar vesicles (15 μg) was measured via quenching of 1 μM 9-amino-6-chloro-2-methoxyacridine (ACMA) upon the addition of 0.5 mM ATP−1 mM $MgSO_4$ (MgATP). Percentage activities are expressed relative to that of BWP17 and are shown as the average ± SD. For n = 3 separate vacuolar purifications, percent reductions in activity are indicated. *p < 0.001 versus BWP17.

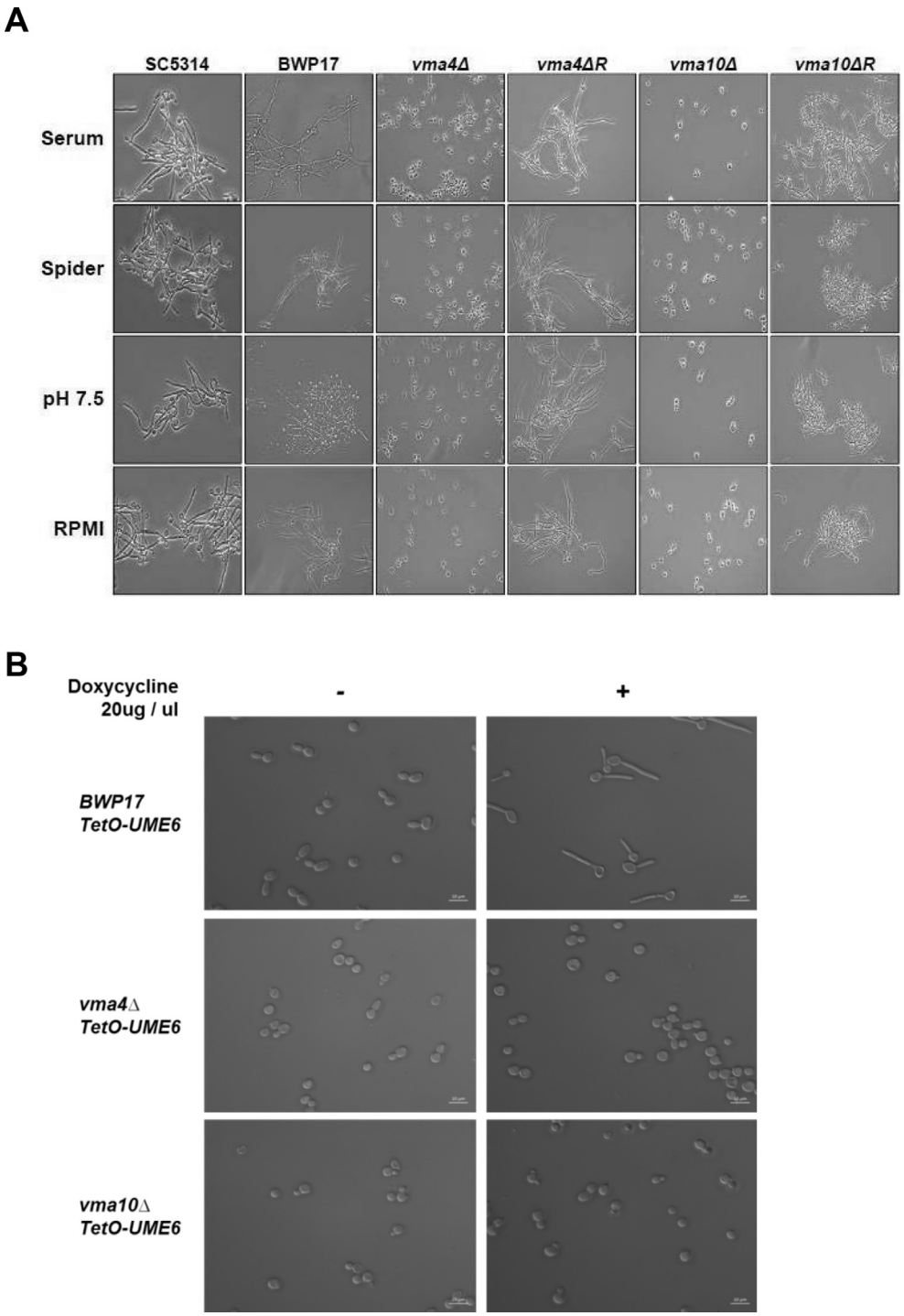

Fig. 5. Vma4 and Vma10 play a role in the morphological transition. (A) Strains (SC5314, BWP17, *vma4Δ*, *vma10Δ*, *vma4ΔR*, and *vma10ΔR*) were cultured overnight and inoculated in various hyphae induction media at an OD_{600} of 1.0. After 2 h of incubation, samples were examined with phase-contrast microscopy. (B) Pre-cultured strains (TetO-UME6 BWP17, TetO-UME6 *vma4Δ*, and TetO-UME6 *vma10Δ*) were incubated for 2 h in YPD medium with or without doxycycline (20 μg/ml).

researchers that several mutants showing abnormal endosomal trafficking and vacuolar functions are also avirulent (Johnston et al., 2009; Palmer et al., 2005). There were also many reports that the Ura3-auxotrophic mutants of *C. albicans* are avirulent in the murine systemic model of candidiasis (Kirsch and Whitney, 1991), so the *URA3* gene was re-integrated into its own DNA locus in BWP17, *vma4Δ* and *vma10Δ* strains. In this study, a systemic candida infection was introduced in mice (n = 10 each) with SC5314, BWP17, *vma4Δ*, *vma10Δ*, *vma4ΔR*, and *vma10ΔR* strains. After a 1-month survival test, none of the mice infected with *vma4Δ* or *vma10Δ* mutants had died. However, BALB/c mice inoculated with SC5314 or BWP17 strains did not survive longer than 2 weeks, with the exception of 1 mouse (Fig. 7). As expected, mice injected with *vma4ΔR* and *vma10ΔR* showed similar virulence effects as the wildtype. These results solidly support the hypothesis that Vma4 and Vma10 are required for the virulence of *C. albicans* by regulating hyphal morphogenesis, protease secretion and acidification of vacuoles.

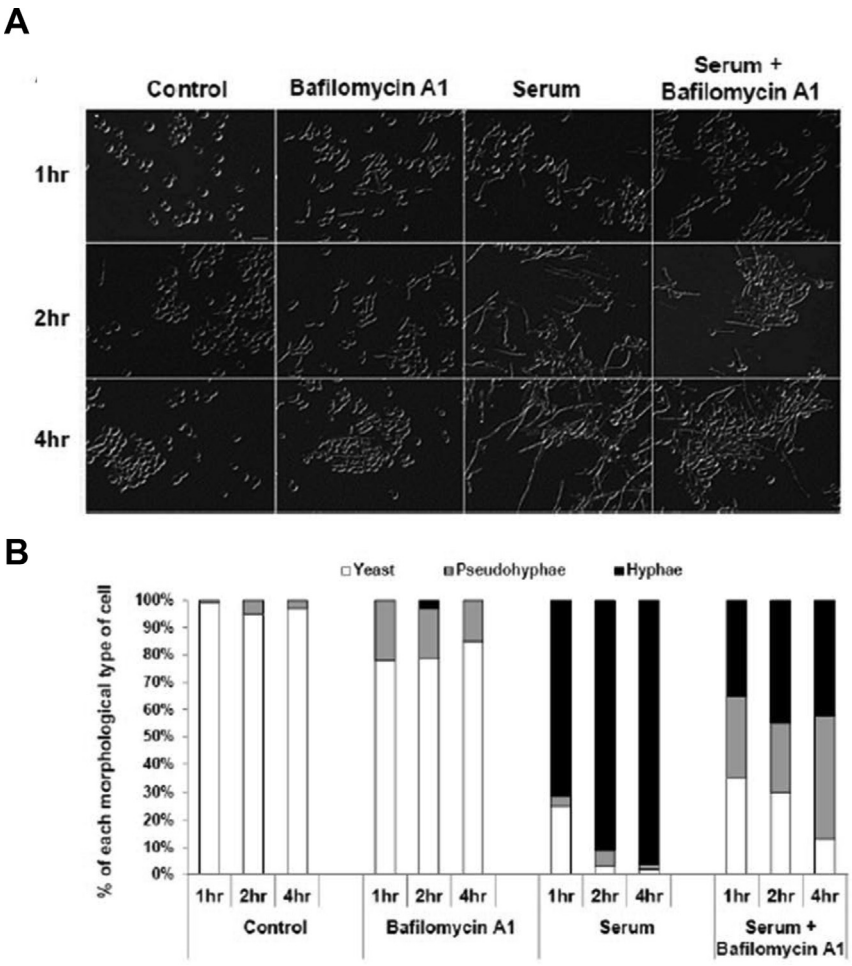

Fig. 6. Vacuolar H^+-ATPase complex (V-ATPase) inhibitor blocks normal hyphae growth. (A) Overnight-cultured SC5314 cells were re-cultured in YPD (control), YPD supplemented with 2 μM bafilomycin A1 (bafilomycin A1), YPD containing 10 % serum (serum), or YPD containing 10 % serum, supplemented with 2 μM bafilomycin A1 (serum + bafilomycin A1). Cell morphology was examined with differential interference contrast microscopy at the indicated time. (B) The number of cells of each morphology type was counted. The percentage of each type of cell was calculated and is presented in the graph. At least 100 cells were counted. Each experiment was performed in triplicate; a representative experiment is shown.

3.8. vma4Δ *and* vma10Δ *cells showed hypersensitivity to antifungal drugs*

Azoles specifically inhibit lanosterol 14α-demethylase (encoded by *ERG11*), block the production of ergosterol, and cause the accumulation of a toxic sterol intermediate, which results in cell membrane malformation (Cowen, 2008; Cui et al., 2015). Since these drugs target the synthesis of membrane-embedded sterol, it was hypothesized that *vma4Δ* and *vma10Δ* mutants defective in vacuole function would be more sensitive to azoles, because ergosterol directly modulates V-ATPase activity (Zhang et al., 2010). Therefore, each strain was spotted on YPD medium containing fluconazole (4 μg/ml), amphotericin B (2 μg/ml), or terbinafine (2 μg/ml) to confirm drug sensitivity. These three antifungal agents are known to kill fungi by inhibiting ergosterol biosynthesis or by binding directly to ergosterol (Odds et al., 2003). Growth was severely diminished only in the *vma4Δ* and *vma10Δ* strains upon supplementation with each drug (Fig. 8A). The Minimum Inhibitory Concentration (MIC) of each drug was also tested (Fig. 8B). The MIC results also showed that *vma4Δ* and *vma10Δ* cells were sensitive to antifungal agents that inhibit the synthesis of sterols or that bind directly to sterols. These results suggest that *vma4* and *vma10* deletion strains have sensitivity in antifungal agents related to ergosterol compared to wild type. The hypersensitivity to antifungal drugs was verified further using V-ATPase inhibitors and basic Kirby–Bauer methods. It was also found that cells treated with the V-ATPase inhibitors, such as 0.5 μM bafilomycin A1 or 1 μM concanamycin A, were more sensitive to fluconazole than those treated with drug vehicle control (DMSO; Fig. 8C). From these observations, it was concluded that Vma4 and Vma10 are essential for the resistance of *C. albicans* against antifungal drugs that inhibit ergosterol biosynthesis. These results strongly indicate that V-ATPase could be a good anti-fungal drug target of *C. albicans*.

4. Discussion

Fungal V-ATPase is critical for cellular functions including vacuole acidification, metal ion detoxification, pH-dependent growth, endosomal transport and trafficking, hyphae growth, and pathogenicity (Parra et al., 2014). In this study, increased expression of Vma4 in cells undergoing hyphae growth was detected through proteomic analyses. In previous studies, Vma4 was reported to interact tightly with Vma10 and they are both present at the V_1 domain of the V-ATPase complex in *S. cerevisiae* (Ohira et al., 2006). Therefore, we focused on the roles of Vma4 and Vma10 during morphological conversion in *C. albicans*. To confirm that levels of

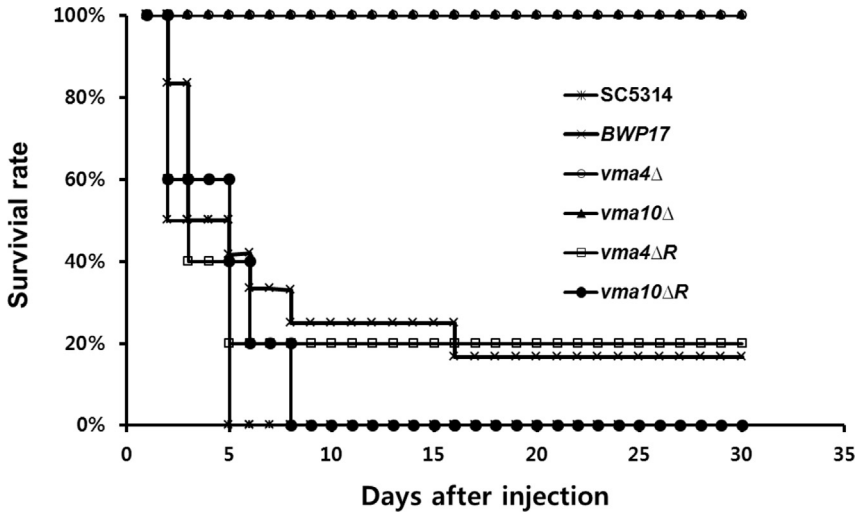

Fig. 7. The vma4Δ and vma10Δ mutants are avirulent in a mouse model. 5-week-old BALB/c mice were inoculated with 1.0×10^6 cells of each strain (SC5314, BWP17, *vma4Δ*, *vma10Δ*, *vma4ΔR*, and *vma10ΔR*) via the lateral tail vein (n = 10 each). The survival of the mice was monitored daily for 1 m.

A

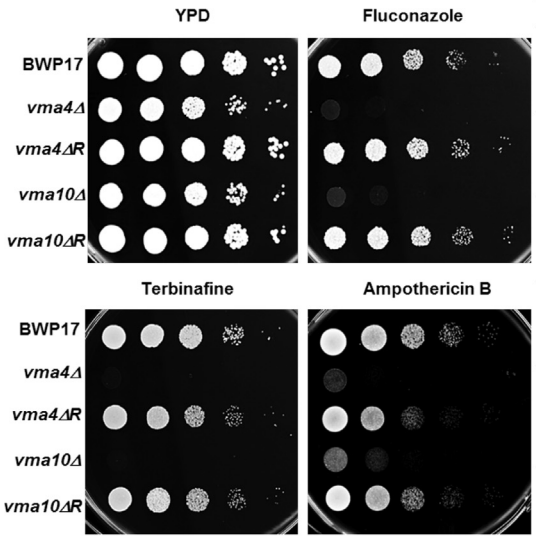

B

Strains	Drugs	MIC (ug/ml)
SC5314	Fluconazole	4
	Amphotericin B	2
	Terbinafine	4
BWP17	Flu	4
	AMB	2
	Ter	4
vma4Δ	Flu	2
	AMB	1
	Ter	0.125
vma10Δ	Flu	1
	AMB	0.5
	Ter	0.125
VMA4ΔR	Flu	4
	AMB	2
	Ter	4
VMA10ΔR	Flu	4
	AMB	1
	Ter	2

C

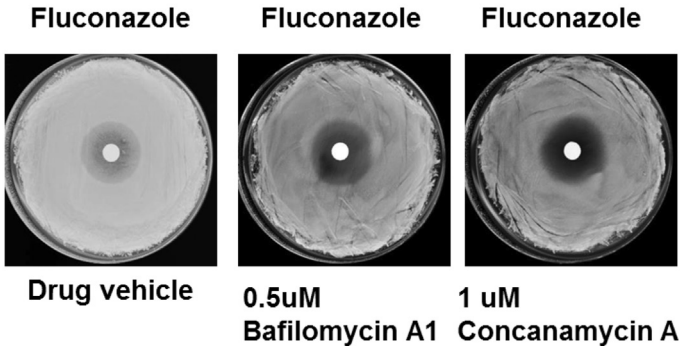

Fig. 8. VMA4 and VMA10 deletion mutants are hypersensitive to antifungal drugs. (A) BWP17, *vma4Δ*, *vma10Δ*, *vma4ΔR* and *vma10ΔR* strains were plated onto YPD agar supplemented with or without fluconazole (4 μg/ml), amphotericin B (2 μg/ml), or terbinafine (2 μg/ml). Images of the plate were taken after 1 d of incubation at 30 °C. (B) The minimum inhibitory concentration for the three antifungal agents against indicated each strain. (C) Approximately 1.0×10^6 overnight-cultured SC5314 cells were smeared on YPD agar harboring vehicle (DMSO) or YPD agar supplemented with 0.5 μM bafilomycin A1 or 1 μM concanamycin A, followed by placing a disc containing fluconazole on the indicated agar plate. Images were captured after 1 d of incubation at 30 °C. Each experiment was performed in triplicate; a representative experiment is shown.

Vma4 and Vma10 are increased in various hyphae growing conditions, Vma4-GFP- and Vma10-GFP-tagged strains were generated and incubated in various hyphal growing conditions. As expected, protein expression of Vma4 and Vma10 was increased in serum, spider medium, and different pH conditions. Therefore, the increase in Vma4 or Vma10 expression is a general phenomenon for hyphal growth, not because of the specific agent used for inducing hyphal growth (Leach et al., 2012; O'Meara and Cowen, 2014; Shapiro and Cowen, 2010).

Why does *C. albicans* require more Vma4 and Vma10 stalk proteins during hyphae growth? During *C. albicans* hyphal growth, vacuole formation occurs extensively (Palmer, 2010; Veses et al., 2009). V-ATPases are located in the cholesterol-rich micro domain of the vacuole membrane. Sterols or membrane proteins are also needed for extensive vacuolation during hyphae growth (Rane et al., 2014). Thus, more V-ATPase subunit proteins such as Vma4 and Vma10 appear to be required for extending the vacuole membrane. Levels of Vma4, which is known to play a potential regulatory role for the catalytic activity of ATPase, appear to increase slightly more than Vma10. This is probably due to the existence of an unstructured area in the C-terminus of the E subunit which is quite unstable and easily degraded (Rishikesan and Gruber, 2011). It is known that the typical *vma*$^-$ phenotypes are sensitive to alkaline pH growth, vacuole fusion defects, metal ion sensitivity, vacuole acidification, and defects in non-fermentable carbon source conditions. From these observations, *vma4Δ* and *vma10Δ* strains appeared to contain the *vma*$^-$ phenotypes as expected. ATP hydrolysis activity and proton transport activity were also defective in *vma4Δ* and *vma10Δ* strains. Previous studies showed that mutations in the Vma7, Vma2, Vph1, Vma3, and Tfp1 subunits of V-ATPase in *C. albicans* also resulted in a similar phenotype (Patenaude et al., 2013; Poltermann et al., 2005; Raines et al., 2013; Rane et al., 2013, 2014). Thus, the stalk region in the V_1 domain also seems to be important for V-ATPase activity, both functionally and structurally. However, Vma4 and Vma10 could be more critical since they are located in the outermost region of the complex.

One novel finding of this study is that Vma4 and Vma10 are required for morphological transition and virulence. In various hyphae-inducing conditions (liquid or solid), *vma4Δ* and *vma10Δ* could not change their morphology from the yeast form to the hyphae form. In a murine systemic infection model of candidiasis, virulence was significantly attenuated in *vma4Δ*- or *vma10Δ*-infected mice. Two possibilities can explain the mechanism of the absolute defect in the virulence of both mutants. First, a defect in the morphological transition may render *C. albicans* avirulent. As previously mentioned, the germ tubes are believed to be required for invading into host tissues and for evading phagocytes such as macrophages (Calderone and Fonzi, 2001; Sudbery, 2011). Second, a defect in endosomal trafficking may affect the expression of membrane proteins that are important for adhesion and invasive activity (Chaffin, 2008; Moreno-Ruiz et al., 2009; Moyes et al., 2016). Moreover, protease secretion was defective in *vma4Δ* and *vma10Δ* strains (Fig. S7). *C. albicans* secretes aspartyl proteinases and lipases that are involved in nutrient acquisition, host cell degradation, and immune evasion (De Bernardis et al., 2001). Thus, this result can explain that the stalk regions of V-ATPase, especially Vma4 and Vma10, may regulate protease activities or secretory vesicles through processing mechanisms. This might be another reason why *vma4Δ and vma10Δ* strains are avirulent.

Another novel finding is that inhibiting V-ATPase activity with bafilomycin A1 or concanamycin A results in a similar phenotype as that of Vma4 and Vma10 deletion strains. Additionally, loss of *VMA4* or *VMA10* results in hypersensitivity to fluconazole, amphotericin B, and terbinafine. Zhang et al. demonstrated a critical requirement for ergosterol in V-ATPase function (Zhang et al., 2010). There is one possibility regarding the inhibitory activity of V-ATPase by fluconazole. It is well known that V-ATPase is associated with the cholesterol-rich microdomain of vacuolar membranes. Fluconazole and other azole drugs can interact with the vacuolar membrane and affect V-ATPase function by restricting its structural flexibility. The alteration of sterol composition caused by inhibiting ergosterol biosynthesis might also affect vacuole membrane packing and rigidity (Abe et al., 2009; Del Poeta et al., 2000). This suggests that V-ATPase-specific inhibitors and ergosterol synthesis inhibitors could have a synergistic effect on *C. albicans* infection when they are simultaneously applied to the pathogenic fungi. Taken together, these proteins could be potential therapeutic targets or a good starting point for developing new anti-fungal drugs for candidiasis.

Acknowledgments

This work was supported by a 2017 NRF2017-R1E1A1A01074101 Grant from the Ministry of Science and Technology, Korea. Consulting service from the MCRB (Seoul, Korea) was kindly appreciated.

Appendix A. Supplementary data

Supplementary data to this article can be found online at https://doi.org/10.1016/j.funbio.2019.06.002.

References

Abe, F., Usui, K., Hiraki, T., 2009. Fluconazole modulates membrane rigidity, heterogeneity, and water penetration into the plasma membrane in Saccharomyces cerevisiae. Biochemistry 48, 8494–8504.
Banerjee, M., Thompson, D.S., Lazzell, A., Carlisle, P.L., Pierce, C., Monteagudo, C., Lopez-Ribot, J.L., Kadosh, D., 2008. UME6, a novel filament-specific regulator of *Candida albicans* hyphal extension and virulence. Mol. Biol. Cell. 19, 1354–1365.
Beyenbach, K.W., Wieczorek, H., 2006. The V-type H+ ATPase: molecular structure and function, physiological roles and regulation. J. Exp. Biol. 209, 577–589.
Calderone, R.A., Fonzi, W.A., 2001. Virulence factors of *Candida albicans*. Trends Microbiol. 9, 327–335.
Chaffin, W.L., 2008. *Candida albicans* cell wall proteins. Microbiol. Mol. Biol. Rev. 72, 495–544.
Chan, C.Y., Prudom, C., Raines, S.M., Charkhzarrin, S., Melman, S.D., De Haro, L.P., Allen, C., Lee, S.A., Sklar, L.A., Parra, K.J., 2012. Inhibitors of V-ATPase proton transport reveal uncoupling functions of tether linking cytosolic and membrane domains of V0 subunit a (Vph1p). J. Biol. Chem. 287, 10236–10250.
Cognetti, D., Davis, D., Sturtevant, J., 2002. The *Candida albicans* 14-3-3 gene, BMH1, is essential for growth. Yeast 19, 55–67.
Cowen, L.E., 2008. The evolution of fungal drug resistance: modulating the trajectory from genotype to phenotype. Nat. Rev. Microbiol. 6, 187–198.
Cui, J., Ren, B., Tong, Y., Dai, H., Zhang, L., 2015. Synergistic combinations of antifungals and anti-virulence agents to fight against *Candida albicans*. Virulence 6, 362–371.
De Bernardis, F., Sullivan, P.A., Cassone, A., 2001. Aspartyl proteinases of *Candida albicans* and their role in pathogenicity. Med. Mycol. 39, 303–313.
Del Poeta, M., Cruz, M.C., Cardenas, M.E., Perfect, J.R., Heitman, J., 2000. Synergistic antifungal activities of bafilomycin A(1), fluconazole, and the pneumocandin MK-0991/caspofungin acetate (L-743,873) with calcineurin inhibitors FK506 and L-685,818 against Cryptococcus neoformans. Antimicrob. Agents Chemother. 44, 739–746.
Duggan, S., Leonhardt, I., Hunniger, K., Kurzai, O., 2015. Host response to *Candida albicans* bloodstream infection and sepsis. Virulence 6, 316–326.
Fishman, J.A., Rubin, R.H., 1998. Infection in organ-transplant recipients. N. Engl. J. Med. 338, 1741–1751.
Fonzi, W.A., Irwin, M.Y., 1993. Isogenic strain construction and gene mapping in *Candida albicans*. Genetics 134, 717–728.
Forgac, M., 2007. Vacuolar ATPases: rotary proton pumps in physiology and pathophysiology. Nat. Rev. Mol. Cell Biol. 8, 917–929.
Hayek, S.R., Lee, S.A., Parra, K.J., 2014. Advances in targeting the vacuolar proton-translocating ATPase (V-ATPase) for anti-fungal therapy. Front. Pharmacol. 5.
Jia, C., Yu, Q.L., Xu, N., Zhang, B., Dong, Y.J., Ding, X.H., Chen, Y.L., Zhang, B., Xing, L.J., Li, M.C., 2014. Role of TFP1 in vacuolar acidification, oxidative stress and filamentous development in *Candida albicans*. Fungal Genet. Biol. 71, 58–67.
Johnston, D.A., Eberle, K.E., Sturtevant, J.E., Palmer, G.E., 2009. Role for endosomal and vacuolar GTPases in *Candida albicans* pathogenesis. Infect. Immun. 77, 2343–2355.

Joo, Y.J., Kim, J.A., Baek, J.H., Seong, K.M., Han, K.D., Song, J.M., Choi, J.Y., Kim, J., 2009. Cooperative regulation of ADE3 transcription by Gcn4p and Bas1p in Saccharomyces cerevisiae. Eukaryot. Cell 8, 1268–1277.
Kim, J., Sudbery, P., 2011. *Candida albicans*, a major human fungal pathogen. J. Microbiol. 49, 171–177.
Kirsch, D.R., Whitney, R.R., 1991. Pathogenicity of candida-albicans auxotrophic mutants in experimental infections. Infect. Immun. 59, 3297–3300.
Klionsky, D.J., Herman, P.K., Emr, S.D., 1990. The fungal vacuole: composition, function, and biogenesis. Microbiol. Rev. 54, 266–292.
Leach, M.D., Klipp, E., Cowen, L.E., Brown, A.J.P., 2012. Fungal Hsp90: a biological transistor that tunes cellular outputs to thermal inputs. Nat. Rev. Microbiol. 10, 693–704.
Li, S.C., Kane, P.M., 2009. The yeast lysosome-like vacuole: endpoint and crossroads. Bba Mol. Cell. Res. 1793, 650–663.
Li, S.X., Wu, H.T., Liu, Y.T., Jiang, Y.Y., Zhang, V.S., Liu, W.D., Zhu, K.J., Li, D.M., Zhang, H., 2018. The F1Fo-ATP synthase beta subunit is required for *Candida albicans* pathogenicity due to its role in carbon flexibility. Front. Microbiol. 9.
Liu, H., 2001. Transcriptional control of dimorphism in *Candida albicans*. Curr. Opin. Microbiol. 4, 728–735.
Lo, H.J., Kohler, J.R., DiDomenico, B., Loebenberg, D., Cacciapuoti, A., Fink, G.R., 1997. Nonfilamentous *C. albicans* mutants are avirulent. Cell 90, 939–949.
Low, C.Y., Rotstein, C., 2011. Emerging fungal infections in immunocompromised patients. F1000 Med. Rep. 3, 14.
Monteoliva, L., Martinez-Lopez, R., Pitarch, A., Hernaez, M.L., Serna, A., Nombela, C., Albar, J.P., Gil, C., 2011. Quantitative proteome and acidic subproteome profiling of *Candida albicans* yeast-to-hypha transition. J. Proteome Res. 10, 502–517.
Moreno-Ruiz, E., Galan-Diez, M., Zhu, W., Fernandez-Ruiz, E., d'Enfert, C., Filler, S.G., Cossart, P., Veiga, E., 2009. *Candida albicans* internalization by host cells is mediated by a clathrin-dependent mechanism. Cell Microbiol. 11, 1179–1189.
Moyes, D.L., Wilson, D., Richardson, J.P., Mogavero, S., Tang, S.X., Wernecke, J., Hofs, S., Gratacap, R.L., Robbins, J., Runglall, M., Murciano, C., Blagojevic, M., Thavaraj, S., Forster, T.M., Hebecker, B., Kasper, L., Vizcay, G., Iancu, S.I., Kichik, N., Hader, A., Kurzai, O., Luo, T., Kruger, T., Kniemeyer, O., Cota, E., Bader, O., Wheeler, R.T., Gutsmann, T., Hube, B., Naglik, J.R., 2016. Candidalysin is a fungal peptide toxin critical for mucosal infection. Nature 532, 64.
O'Meara, T.R., Cowen, L.E., 2014. Hsp90-dependent regulatory circuitry controlling temperature-dependent fungal development and virulence. Cell Microbiol. 16, 473–481.
Odds, F.C., Brown, A.J.P., Gow, N.A.R., 2003. Antifungal agents: mechanisms of action. Trends Microbiol. 11, 272–279.
Ohira, M., Smardon, A.M., Charsky, C.M., Liu, J., Tarsio, M., Kane, P.M., 2006. The E and G subunits of the yeast V-ATPase interact tightly and are both present at more than one copy per V1 complex. J. Biol. Chem. 281, 22752–22760.
Olsen, I., 2014. Attenuation of *Candida albicans* virulence with focus on disruption of its vacuole functions. J. Oral Microbiol. 6.
Oot, R.A., Wilkens, S., 2010. Domain characterization and interaction of the yeast vacuolar ATPase subunit C with the peripheral stator stalk subunits E and G. J. Biol. Chem. 285, 24654–24664.
Owegi, M.A., Pappas, D.L., Finch Jr., M.W., Bilbo, S.A., Resendiz, C.A., Jacquemin, L.J., Warrier, A., Trombley, J.D., McCulloch, K.M., Margalef, K.L., Mertz, M.J., Storms, J.M., Damin, C.A., Parra, K.J., 2006. Identification of a domain in the V0 subunit d that is critical for coupling of the yeast vacuolar proton-translocating ATPase. J. Biol. Chem. 281, 30001–30014.
Palmer, G.E., 2010. Endosomal and AP-3-dependent vacuolar trafficking routes make additive contributions to *Candida albicans* hyphal growth and pathogenesis. Eukaryot. Cell 9, 1755–1765.
Palmer, G.E., Kelly, M.N., Sturtevant, J.E., 2005. The *Candida albicans* vacuole is required for differentiation and efficient macrophage killing. Eukaryot. Cell 4, 1677–1686.
Park, N.H., Choi, W., 2002. Vectors designed for efficient molecular manipulation in *Candida albicans*. Yeast 19, 1057–1066.
Parra, K.J., Chan, C.Y., Chen, J., 2014. Saccharomyces cerevisiae vacuolar H+-ATPase regulation by disassembly and reassembly: one structure and multiple signals. Eukaryot. Cell 13, 706–714.
Patenaude, C., Zhang, Y., Cormack, B., Kohler, J., Rao, R., 2013. Essential role for vacuolar acidification in *Candida albicans* virulence. J. Biol. Chem. 288, 26256–26264.
Pfaller, M.A., Diekema, D.J., 2007. Epidemiology of invasive candidiasis: a persistent public health problem. Clin. Microbiol. Rev. 20, 133–163.
Poltermann, S., Nguyen, M., Gunther, J., Wendland, J., Hartl, A., Kunkel, W., Zipfel, P.F., Eck, R., 2005. The putative vacuolar ATPase subunit Vma7p of *Candida albicans* is involved in vacuole acidification, hyphal development and virulence. Microbiology 151, 1645–1655.
Raines, S.M., Rane, H.S., Bernardo, S.M., Binder, J.L., Lee, S.A., Parra, K.J., 2013. Deletion of vacuolar proton-translocating ATPase V(o)a isoforms clarifies the role of vacuolar pH as a determinant of virulence-associated traits in *Candida albicans*. J. Biol. Chem. 288, 6190–6201.
Rane, H.S., Bernardo, S.M., Hayek, S.R., Binder, J.L., Parra, K.J., Lee, S.A., 2014. The contribution of *Candida albicans* vacuolar ATPase subunit V1B, encoded by VMA2, to stress response, autophagy, and virulence is independent of environmental pH. Eukaryot. Cell 13, 1207–1221.
Rane, H.S., Bernardo, S.M., Raines, S.M., Binder, J.L., Parra, K.J., Lee, S.A., 2013. *Candida albicans* VMA3 is necessary for V-ATPase assembly and function and contributes to secretion and filamentation. Eukaryot. Cell 12, 1369–1382.
Rishikesan, S., Gruber, G., 2011. Structural elements of the C-terminal domain of subunit E (E133-222) from the Saccharomyces cerevisiae V1VO ATPase determined by solution NMR spectroscopy. J. Bioenerg. Biomembr. 43, 447–455.
Santos, G.C.D., Vasconcelos, C.C., Lopes, A.J.O., Cartagenes, M.D.D., Filho, A.K.D.B., do Nascimento, F.R.F., Ramos, R.M., Pires, E.R.R.B., de Andrade, M.S., Rocha, F.M.G., Monteiro, C.D., 2018. Candida infections and therapeutic strategies: mechanisms of action for traditional and alternative agents. Front. Microbiol. 9.
Schmitt, M.E., Brown, T.A., Trumpower, B.L., 1990. A rapid and simple method for preparation of RNA from Saccharomyces cerevisiae. Nucleic Acids Res. 18, 3091–3092.
Shao, E., Forgac, M., 2004. Involvement of the nonhomologous region of subunit A of the yeast V-ATPase in coupling and *in vivo* dissociation. J. Biol. Chem. 279, 48663–48670.
Shapiro, R.S., Cowen, L., 2010. Coupling temperature sensing and development: hsp90 regulates morphogenetic signalling in *Candida albicans*. Virulence 1, 45–48.
Sudbery, P.E., 2011. Growth of *Candida albicans* hyphae. Nat. Rev. Microbiol. 9, 737–748.
Teter, S.A., Klionsky, D.J., 2000. Transport of proteins to the yeast vacuole: autophagy, cytoplasm-to-vacuole targeting, and role of the vacuole in degradation. Semin. Cell Dev. Biol. 11, 173–179.
Veses, V., Richards, A., Gow, N.A., 2009. Vacuole inheritance regulates cell size and branching frequency of *Candida albicans* hyphae. Mol. Microbiol. 71, 505–519.
Vida, T.A., Emr, S.D., 1995. A new vital stain for visualizing vacuolar membrane dynamics and endocytosis in yeast. J. Cell Biol. 128, 779–792.
Walther, A., Wendland, J., 2008. PCR-based gene targeting in *Candida albicans*. Nat. Protoc. 3, 1414–1421.
Wilson, R.B., Davis, D., Enloe, B.M., Mitchell, A.P., 2000. A recyclable *Candida albicans* URA3 cassette for PCR product-directed gene disruptions. Yeast 16, 65–70.
Wilson, R.B., Davis, D., Mitchell, A.P., 1999. Rapid hypothesis testing with *Candida albicans* through gene disruption with short homology regions. J. Bacteriol. 181, 1868–1874.
Zhang, J.W., Parra, K.J., Liu, J., Kane, P.M., 1998. Characterization of a temperature-sensitive yeast vacuolar ATPase mutant with defects in actin distribution and bud morphology. J. Biol. Chem. 273, 18470–18480.
Zhang, Y.Q., Gamarra, S., Garcia-Effron, G., Park, S., Perlin, D.S., Rao, R., 2010. Requirement for ergosterol in V-ATPase function underlies antifungal activity of azole drugs. PLoS Pathog. 6, e1000939.